

# Mapping vertical profile of discontinuous permafrost with ground penetrating radar at Nalaikh depression, Mongolia

Tonghua Wu · Qinxue Wang · Masataka Watanabe ·  
Ji Chen · Dorjgotov Battogtokh

Received: 5 November 2007 / Accepted: 18 February 2008 / Published online: 15 March 2008  
© Springer-Verlag 2008

**Abstract** Ground-penetrating radar (GPR) has become an important geophysical tool which can provide a wealth of interpretive information about the vertical profile of discontinuous permafrost. A GPR investigation was conducted in October 2006 at the Nalaikh site at the southern boundary of the Siberian discontinuous permafrost region in Mongolia. GPR data were collected along four 100-m-long profiles to identify the location of the permafrost body, which included an in situ drilling borehole and analysis of temperature observations and soil water content measurements from boreholes. The GPR interpretation results indicated that the thickness of discontinuous permafrost at the study site was only 1.9–3.0 m and the permafrost is vulnerable to climate change. The soil temperature and soil

water content data demonstrate the precision of GPR image interpretation. This case demonstrated that GPR is well suited for mapping the internal structure of discontinuous permafrost with relatively low soil water content.

**Keywords** Discontinuous permafrost · Ground-penetrating radar · Vertical profile · Permafrost degradation

## Introduction

Permafrost is defined as ground that remains at or below 0°C for two or more years (Muller 1947). It is widespread in high latitudes and at high elevations regions (Zhang et al. 2007). Permafrost occupies about a quarter of the terrestrial northern hemisphere (Zhang et al. 1999). Most of recent studies indicate that the extent of permafrost has been decreasing worldwide due to global warming (Harris et al. 2003; Sazonova et al. 2004; Osterkamp 2005; Cheng and Wu 2007). Permafrost degradation will exert a great impact on the local hydrology, land desertification, ecology, design of buildings and even feedback to climate (Woo and Winter 1993; Jorgenson et al. 2001; Nelson et al. 2001; Atsuko et al. 2002; Yang et al. 2004; Woo and Marsh 2005; Laroocque et al. 2006). The climate of Mongolia is characterized by a long cold winter and a short warmer summer (Bereneva 1992), and the ground in northern Mongolia is extensively underlain by permafrost. Mongolia is situated at the southern boundary of the Siberian cryosphere, and the permafrost region accounts for approximately two-thirds of the territory of this country (Sharkhuu 2003). Thus, the existence of permafrost is an important consideration for environmental studies in Mongolia. Most borehole profiles have displayed a tendency toward warming of the ground temperature in

---

T. Wu · Q. Wang (✉)  
Asia Water Environment Section,  
Asian Environmental Research Group,  
National Institute for Environmental Studies,  
16-2 Onogawa, Tsukuba 305-8506, Japan  
e-mail: wangqx@nies.go.jp

T. Wu  
Cryosphere Research Station on the Qinghai-Tibet Plateau,  
State Key Laboratory of Cryospheric Science,  
Chinese Academy of Sciences, 730000 Lanzhou, China

M. Watanabe  
Faculty of Environmental Information, Keio University,  
5522 Endo, Fujisawa, Kanagawa 252-8520, Japan

J. Chen  
Cold and Arid Regions Environmental and Engineering  
Research Institute, Chinese Academy of Sciences,  
730000 Lanzhou, China

D. Battogtokh  
Institute of Geography, Mongolian Academy of Sciences,  
Ulaanbaatar 210620, Mongolia

Mongolia according to observations during the past 40 years (Sharkhuu and Sharkhuu 2005). It is important to acquire knowledge of the internal composition and structure of permafrost to assess its dynamic response to climatic changes.

Conventionally, the direct method to identify the vertical profile of permafrost is to drill boreholes, and test pit excavations also can provide detailed information about the shallower ground surface less than 3 m deep. However, these methods are slow, labor intensive, disturb the thermal regime of the soil and sample only certain points. Ground penetrating radar (GPR) is a geophysical method that can provide high resolution three-dimensional images of the subsurface of the earth. GPR has significantly improved the efficiency of the fieldwork that is fundamental to the environmental surveys and the rapid growth of GPR technology during the past 20 years has resulted in its extensive use in environmental investigations (Davis and Annan 1989; Vaughan et al. 1999; Singh and Chauhan 2002; Splajt et al. 2003; Koralay et al. 2007). In most cases, GPR has been demonstrated to be a useful tool for mapping the near-surface thermal structure and stratigraphy of permafrost (Doolittle et al. 1990; Gruber and Ludwig 1996; Arcone et al. 1998; Robinson et al. 2000; Hinkel et al. 2001; Moorman et al. 2003; Bradford et al. 2005; Wu et al. 2005; Jørgenson and Andreasen 2007). Moreover, GPR is also a non-invasive method of subsurface remote sensing for the detection of permafrost in cold regions. Compared with the borehole drilling method, GPR techniques are faster, more portable and provide linear samples.

The purpose of this study was to identify the internal structure of the discontinuous permafrost at the Nalaikh depression in southeast Ulaanbaatar, Mongolia, by means of ground penetrating radar surveys. In conjunction with borehole data, we obtained information about the internal structure of the permafrost body in this region.

### Study site

The study site is located on a flat semiarid pasture plain at the Nalaikh depression in northeastern Mongolia at 47°45'N, 107°20'E, 1,421 m a.s.l. which is about 40 km southeast of Ulaanbaatar (Fig. 1). An automatic weather station (AWS) was established by the Institute of Observational Research for Global Change, Japan Agency for Marine-Earth Science and Technology (IORGC, JAMSTEC) to measure air temperature, humidity and wind speed at the heights of 0.5, 1.0, 2.0 and 4.0 m. The data recorded from July 2002 to June 2004 showed that the mean annual air temperature, relative humidity, and wind speed at this site were  $-4.1^{\circ}\text{C}$ , 61% and 2.6 m/s, respectively. The amount of annual precipitation was 159.8 mm, 79% of

which fell between May and September (Zhang et al. 2005). The superficial geology consists of sand and loam with some gravel with little organic matter. The soil porosity in the surface layer (0–60 cm) ranges from 34 to 58%, and the soil moisture at the depth of 0–50 cm ranges from 6.5 to 17.2%. The ground surface is dry, and vegetation is uniformly sparse grass covering 38–60% of the land surface in summer. The ground surfaces are covered by grass with a maximum height in mid-July of less than 20 cm (Zhang et al. 2004). The study area is situated in an insular and sparsely insular permafrost region (Fig. 1), which was designated a discontinuous permafrost region according to the classification system of the International Permafrost Association (Brown et al. 1997). Ishikawa et al. (2006) observed that the permafrost temperature in the borehole of the automatic weather station was approximately  $0^{\circ}\text{C}$  and that the active layer above the permafrost surface at this site was very dry. The dry active layer offers optimal soil conditions for GPR investigation in that the radar signals are strongly attenuated in soils with high moisture content (Arcone and Delaney 1982).

### Equipment and methods

The sharp contrast between the dielectric constants of ice ( $k = 3\text{--}4$ ), water ( $k = 80$ ), soils ( $k = 5\text{--}40$ ) and air

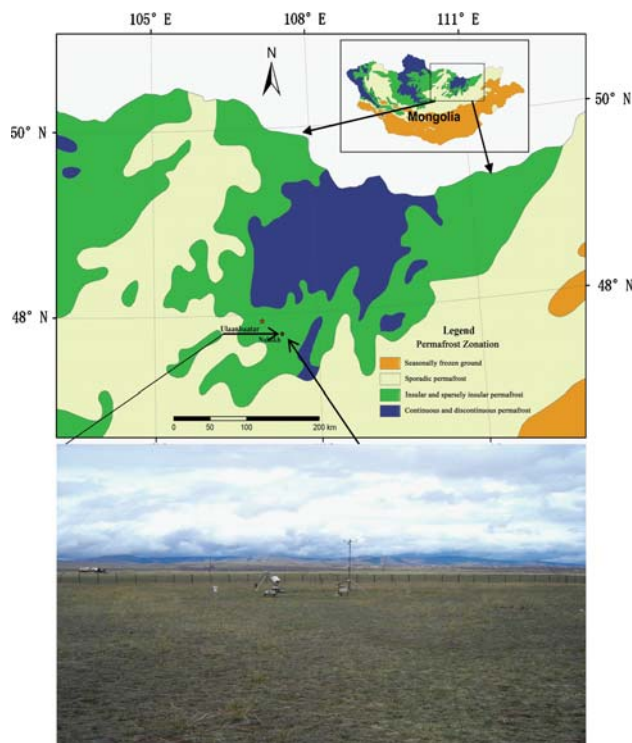


**Fig. 1** A map of the Nalaikh depression and permafrost distribution in this region (after Sodnom and Yanshin 1990)

( $k = 1$ ) makes GPR well suited for mapping the vertical profile of permafrost. The variations in electrical properties due to the differences in soil temperature and moisture lead to different reflection signals in the graph of the GPR profiles. As a result, GPR can be an effective tool to determine the interface between frozen and thawed soil layers. The principle of GPR is to send short pulses of electromagnetic energy into the ground by a transmitting antenna that is placed on the ground surface. A receiving antenna detects the electromagnetic wave signals that are reflected up to the ground surface when the transmitted pulse encounters a subsurface interface across which an electromagnetic impedance contrast exists. The delay between the transmitted pulse and the arrival of a reflection is proportional to the depth of the subsurface feature that generated the reflection (Annan and Davis 1976; Davis et al. 1989). Figure 2 is a schematic diagram that shows the probing principle and components of the GPR system. The GPR system consists of a laptop computer, control panel, transmitter and receiver (Fig. 2). The control panel is connected to the laptop computer with a communication cable and to the transmitter and receiver with optical fibers.

We used a portable, battery-powered Pulse EKKO-100 GPR system (Manufactured by Sensors and Software Inc., Canada) with a central frequency range of 100 MHz. The survey was conducted on 27 October 2006, when there was a snow cover whose thickness ranged from 2 to 5 cm. The equipment was carried by three persons and data were collected parallel to the profile direction. Four profiles whose length was about 100 m were obtained in two perpendicular directions about 30 m away from the square-shaped AWS fence. The antennas were separated by 1 m with two wooden sticks and were oriented broadside to the survey direction (Fig. 2). The GPR measurement parameters are listed in Table 1. The average velocity calculated for time-to-depth conversion was 0.070 m/ns, which was obtained from the relative permittivity, velocity and attenuation of wet sandy soil, as summarized by Daniels (2004). Two-way travel times are converted to depth with the calculated average velocity (0.070 m/ns). Based on the

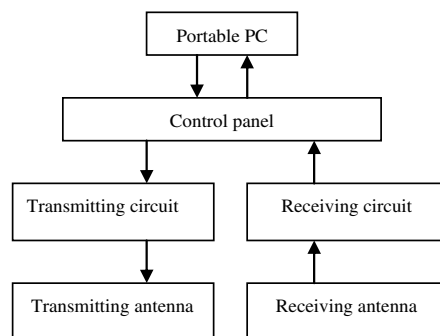
**Table 1** GPR data acquisition parameters

Impulse power	400 V
Center frequency of antennas	100 MHz
Length of antennas	1.0 m
Measurement step	1.0 m
Recording time window	400 ns
Sampling interval	800 ps
Number of stacks	32
Battery power supply	12 V

quarter wavelength theory (Widess 1973), the theoretical vertical resolution of the GPR measurement with a 100 MHz antenna is about 0.2 m. At the time we conducted the GPR investigation, a 7-m-deep borehole was being drilled 20 m away from the Profile 1 by the Geo-Ecology Institute of the Mongolian Academy of Sciences. Soil cores were collected to measure the soil water content and to verify radar interpretation.

The GPR raw data were processed in gray scale formats using PulseEKKO™ software (version 4.22 provided by Sensors and Software Inc., Canada). The post-processing procedures included automatic gain control (AGC), time variable gain, band-pass filtering and DEWOW processing. AGC was used to increase the amplitude of the air and ground wave at large antenna separations in order to compensate for the attenuation of the GPR signal with increasing depth. A time variable gain function applied to the raw data intensifies the signal amplitude with increasing travel time, which enhances stratigraphic detail throughout the profile. Band-pass filtering was applied to improve the signal-to-noise ratio by filtering the frequency bandwidth to include only those frequencies that contain real signal information, and to exclude those frequencies that mainly contain noise. In addition, a DEWOW procedure was applied to remove the low-frequency noise introduced from the finite sampling frequency of the receiver and the inductive effects of the radar equipment.

**Fig. 2** Probing principle and components of GPR



## Results and discussion

The interpretation of GPR images depends predominantly on the difference between reflected electromagnetic wave features of the frozen and thawed layers. Figure 3 shows two representative GPR profiles across the study site. In both profiles, the vertical scale depth is expressed in meters. On account of the relatively strong attenuation of the thick active layer, the penetration of four profiles was much shallower than expected, with a maximum depth of about 10 m (Fig. 3). The interpreted images indicated that the GPR reflections resolved the stratigraphic interface between the frozen and thawed layers, especially the location of the permafrost body. In both figures, the continuous horizontal bands at the top of the GPR profile were interpreted as surface snow. The difference between the radar signals of the sand and loam layer and the sand and gravel layer was relatively small, but we can identify their interfaces by the calibration to in situ drilling cores. The clearest interface in the lower part of both radar profiles was the location of permafrost table which was marked between the sand and gravel layer and the permafrost body. These features are particularly apparent in the interpreted images.

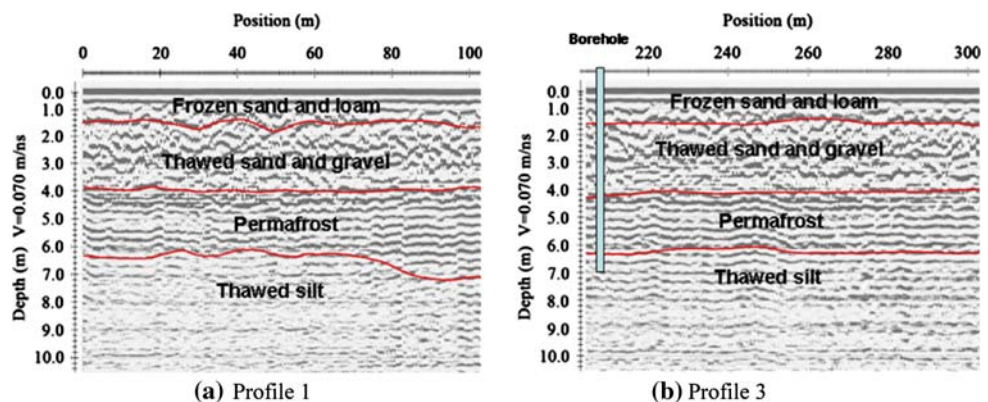
Based on the interpreted GPR images and judged by the sampling soil cores from the in situ drilling borehole, the subsurface was divided into four layers: frozen sand and loam, thawed sand and gravel, permafrost and thawed silt (Fig. 3). The composition of the subsurface stratigraphy was mainly determined by the in situ drilling. Based on the interpretation of all four GPR profiles, we sketched the stratigraphic map of the subsurface (10 m deep) at the study site. Figure 4 indicates that the ground surface started to freeze downward from a depth of 1.2–1.8 m. The permafrost table was located at a depth of 3.8–4.1 m and the permafrost base at a depth of 6.0–6.8 m. The thickness of the permafrost is about 1.9–3.0 m (Fig. 4). The thawed silt layer was estimated to contain a large amount of unfrozen water because of the radar signal was suddenly weakened.

The interpreted GPR images indicated that the composition and structure of each layer were homogeneous and no drastic variations were observed all along the four profiles.

The sampled soil core information, soil temperature and soil water content data can improve our ability to interpret the GPR images and to evaluate the precision of identification made on the radar graphic profiles. The temperature observation data from a 7-m-deep borehole at the starting point of Profile 3 (Fig. 3) correlate well with the GPR interpretation results of the general stratigraphy at the study site. The 7-m-deep borehole was drilled in the spring of 2005 and seven thermistor sensors were placed in the borehole at intervals of 1 m to measure the soil temperature of each depth. The data were collected monthly at the beginning of the month from May 2005 to April 2006. It was concluded from the monthly ground temperature profile during a year that the permafrost table was located at the depth of 4.0–5.0 m (Fig. 4). The ground surface temperature at the beginning of November 2005 was  $-9.54^{\circ}\text{C}$ . The soil temperature at the depth of 7 m was very close to  $0^{\circ}\text{C}$  (Table 2). The temperature data show good accordance with the GPR interpretation results. Ishikawa et al. (2005) reported that the ground temperature remained 0 to  $-0.2^{\circ}\text{C}$  from the depth of 5.3–12 m and slightly above  $0^{\circ}\text{C}$  below 12 m in a 30-m-deep borehole at Nalaikh AWS site (Fig. 5).

In addition, a 7-m-deep borehole was drilled at a site 20 m away from Profile 1 when we conducted our GPR investigation. The ground surface condition of the in situ borehole site was similar to that of the study region. The soil cores were sampled at intervals of 20 cm from the ground surface downward to the depth of 7 m, and the gravimetric soil water content of each sample was measured in the laboratory. Figure 6 shows the gravimetric soil water content at each depth of the in situ borehole site. The gravimetric soil water contents at the surface (0–3 m) were less than 6.0% which demonstrated a dry active layer in the discontinuous permafrost regions. As the depth extends downward, the soil water contents increased gradually

**Fig. 3** Interpreted 100 MHz GPR images along with two representative profiles. The distance between the antennas was 1 m and trace spacing was 10 m. An average propagation velocity of 0.070 m/ns was applied for time to depth conversion. The red lines indicate the interfaces of different soil layers especially the frozen and thawed layer. A 7-m-deep borehole, which was drilled in 2005, is situated at the starting point of Profile 3



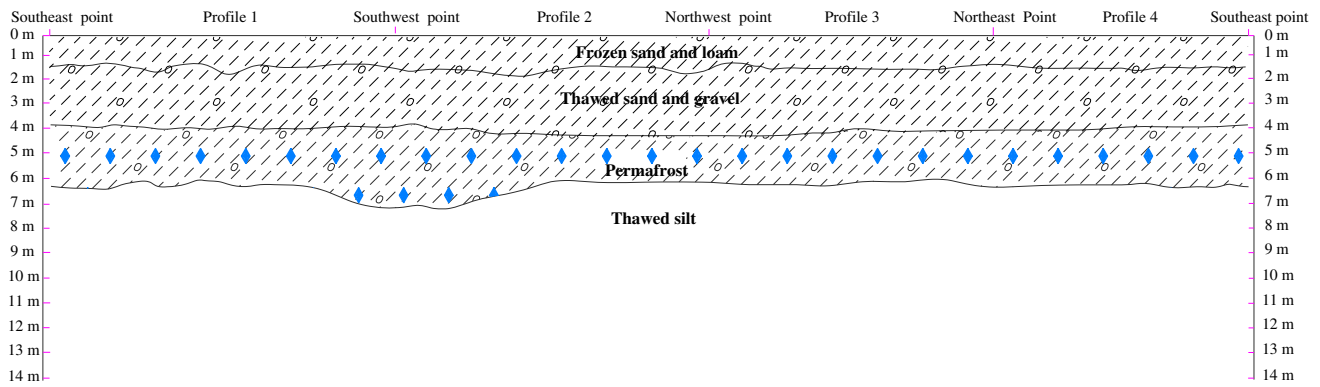


**Fig. 4** The interpreted GPR results of four profiles of the study site. The subsurface was divided into four layers: frozen sand and loam, thawed sand and gravel, permafrost, and thawed silt. The locations of the interfaces between the four layers are sketched in the graph

**Table 2** Ground temperatures data from May 2005 to April 2006

Month	Depth (m)							
	0.0	1.0	2.0	3.0	4.0	5.0	6.0	7.0
May 2005	13.81	1.50	-1.00	-1.15	-0.66	-0.21	-0.10	-0.10
June 2005	19.23	5.78	1.06	-0.52	-0.41	-0.31	-0.13	-0.12
July 2005	23.34	9.73	4.13	0.16	-0.27	-0.34	-0.19	-0.15
August 2005	19.48	10.97	6.25	2.09	-0.14	-0.30	-0.17	-0.13
September 2005	10.05	8.92	6.33	3.32	0.39	-0.21	-0.12	-0.09
October 2005	1.99	4.97	4.40	2.92	1.11	-0.12	-0.08	-0.06
November 2005	-9.54	0.46	1.70	1.62	0.92	-0.10	-0.02	-0.04
December 2005	-20.30	-4.95	-0.64	0.29	0.33	-0.09	0.01	-0.06
January 2006	-23.29	-9.32	-3.58	-0.10	0.19	-0.09	0.02	-0.06
February 2006	-20.70	-10.97	-5.69	-1.41	0.19	-0.09	0.02	-0.06
March 2006	-7.03	-7.77	-5.33	-2.38	0.03	-0.10	-0.02	-0.07
April 2006	0.79	-3.22	-2.97	-1.83	-0.41	-0.11	-0.06	-0.09

from 6 to 10% at the depth of 3–4 m. The soil water contents below the depth of 4 m averaged 8%, which indicated the existence of poor-ice permafrost at the study site. The soil water content measurement data also show a good conformity with the interpreted GPR images.

On the basis of long-term ground temperatures data collected from 1969 to 2002 at a borehole in southern Nalaikh in the vicinity of the study site, Sharkhuu (2003) concluded that the ground temperature was increasing at a rate of 0.01°C/year. According to this estimation, inferred from the detailed interpretation of the GPR reflection profiles, the permafrost at the Nalaikh site is vulnerable to climate change and tends to undergo severe degradation under the scenarios of climate warming and increasing anthropological activities. Ishikawa et al. (2005) predicted that the permafrost at the study site would disappear completely in 20 years. The permafrost degradation will exert great influence on the land-surface hydrological

cycles as well as the exacerbation of grassland degradation in the discontinuous permafrost region.

**Conclusions**

In this study, the GPR technique was used to determine the vertical profile of discontinuous permafrost on a flat pasture plain in Nalaikh, Mongolia. By utilizing the fundamental principle of radar stratigraphy and analyzing the reflected features of frozen and thawed layer, we interpreted our GPR images to demonstrate the location of the permafrost body. The temperature observation data from a drilled borehole throughout the year and the soil water content data from an in situ drilled borehole were generally consistent with the GPR interpretation results. GPR prospecting is very efficient for describing in detail the vertical profile of discontinuous permafrost with

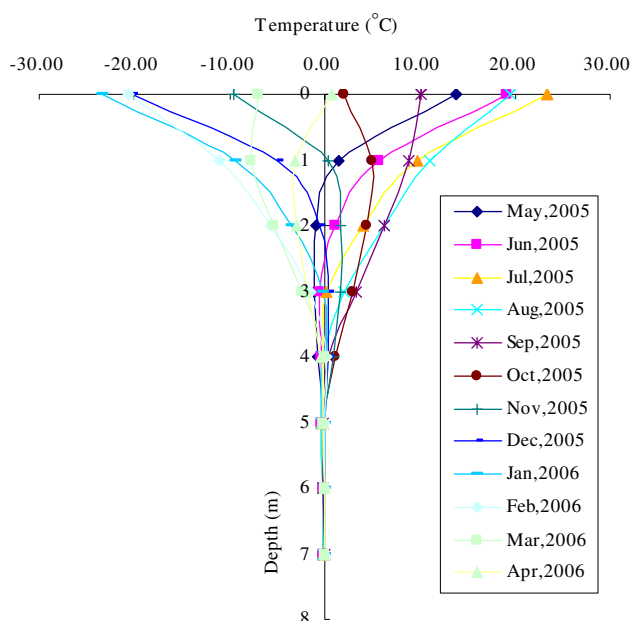


**Fig. 5** Ground temperatures at 1-month-intervals from May 2005 to April 2006. The borehole is located at the starting point of Profile 3

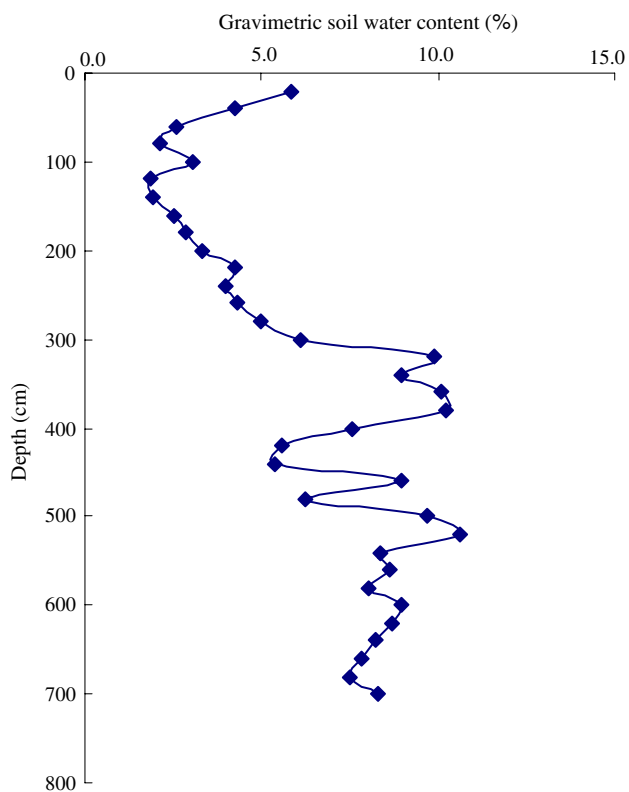


**Fig. 6** Gravimetric moisture at the in situ drilling borehole. The increase of gravimetric moisture content from the depth of 3–7 m downward implies the existence of poor ice in this layer

relatively low soil water content. It seems particularly useful for identifying the location of the permafrost body combined with the validation of the in situ drilling borehole

and soil temperatures measurements. This case also showed that the GPR can serve as a reliable tool for detecting the vertical profile of discontinuous permafrost in two dimensions.

The GPR interpretation results indicated that the permafrost table was located at a depth of 3.8–4.1 m and that the permafrost base at a depth of 6.0–6.8 m in the Nalaikh site. The discontinuous permafrost in the study site was thin and prone to severe degradation. Further study of permafrost degradation could be conducted in the light of the GPR results in this case.

**Acknowledgments** The study conducted in this paper is funded by “the Project of Establishment of Early Observation Network for the Impacts of Global Warming”. We also would like to thank Dr. Ochirbat Batkhisig, Dr. Ya. Jambaljav, and all other staff from Institute of Geography, Mongolian Academy of Sciences for their invaluable logistic support.

## References

- Annan AP, Davis JL (1976) Impulse radar sounding in permafrost. *Radio Sci* 11:383–394
- Arcone SA, Delaney AJ (1982) Dielectric properties of thawed active layers overlying permafrost using radar at VHF. *Radio Sci* 17:618–626
- Arcone SA, Chacho EF, Delaney AJ (1998) Seasonal structure of taliks beneath Arctic streams determined with ground-penetrating radar. In: *Permafrost seventh international conference proceedings*. Yellowknife, Canada, pp 19–24
- Atsuko S, Yanagisawa N, Naito D, Fujita N, Maximov TC (2002) Importance of permafrost as a source of water for plants in east Siberian taiga. *Ecol Res* 17:493–503
- Bereneva IA (1992) Peculiarities of studies and methods of assessment of climatic resources of complex ecosystems of Mongolia. In: *Ecology and nature management in Mongolia (In Russian)*. GuGK, Moscow, pp 25–32
- Bradford JH, McNamara JP, Bowden W, Gooseff MN (2005) Measuring thaw depth beneath peat-lined arctic streams using ground-penetrating radar. *Hydrol Processes* 19:2689–2699
- Brown J, Ferrians O, Heginbottom J, Melnikov E (1997) Circumarctic map of permafrost and ground-ice conditions. US Geological Survey Circum-Pacific Map Ser., Map CP-45, 1:10000000. US Geological Survey, Reston
- Cheng G, Wu T (2007) Responses of permafrost to climate change and their environmental significance, Qinghai-Tibet Plateau. *J Geophys Res* 112:F02S03. doi:10.1029/2006JF000631
- Daniels DJ (2004) *Ground penetrating radar*, 2nd edn. IEE Radar, Sonar and Navigation series 15. The Institution of Electrical Engineers, London. ISBN 0-86341-360-9
- Davis JL, Annan AP (1989) Ground-penetrating radar for high-resolution mapping of soil and rock stratigraphy. *Geophys Prospect* 37:531–551
- Doolittle JA, Hardisky MA, Gross MF (1990) A ground-penetrating radar study of active-layer thicknesses in areas of moist sedge and wet sedge tundra near Bethel, Alaska, USA. *Arct Alp Res* 22:175–182
- Gruber S, Ludwig F (1996) Application of ground penetrating radar in glaciology and permafrost prospecting. Arctic Center, University of Lapland, Lapland. [http://www.ulapland.fi/home/hkunta/jmoore/gpr\\_cryo.pdf](http://www.ulapland.fi/home/hkunta/jmoore/gpr_cryo.pdf)

- Harris C, Daniel VM, Isaksen K, Haeberli W, Sollid JL, King L, Holmlund P, Dramis F, Guglielmin M, Palacios D (2003) Warming permafrost in European mountains. *Glob Planet Change* 39:215–225
- Hinkel KM, Doolittle JA, Bockheim JG, Nelson FE, Paetzold R, Kimble JM, Travis R (2001) Detection of subsurface permafrost features with ground-penetrating radar, Barrow, Alaska. *Permafrost Periglacial Processes* 12:179–190
- Ishikawa M, Sharkhuu N, Zhang Y, Kadota T, Ohata T (2005) Ground thermal and moisture conditions at the southern boundary of discontinuous permafrost, Mongolia. *Permafrost Periglacial Process* 16:209–216
- Ishikawa M, Zhang Y, Kadota T, Ohata T (2006) Hydrothermal regimes of the dry active layer. *Water Resour Res* 42:W04401. doi:10.1029/2005WR004200
- Jørgensen AS, Andreassen F (2007) Mapping of permafrost surface using ground-penetrating radar at Kangerlussuaq airport, western Greenland. *Cold Reg Sci Technol* 48:64–72
- Jorgenson MT, Racine CH, Walters JC, Osterkamp TE (2001) Permafrost degradation and ecological changes associated with a warming climate in central Alaska. *Clim Change* 48(4):551–571
- Koralay T, Kadioglu S, Kadioglu YK (2007) A new approximation in determination of zonation boundaries of ignimbrite by ground penetrating radar: Kayseri, Central Anatolia, Turkey. *Environ Geol* 52:1387–1397
- Larocque GR, Boutin R, Paré D, Robitaille G, Lacerte V (2006) Assessing a new soil carbon model to simulate the effect of temperature increase on the soil carbon cycle in three eastern Canadian forest types characterized by different climatic conditions. *Can J Soil Sci* 86:187–202
- Moorman BJ, Robinson SD, Burgess MM (2003) Imaging periglacial conditions with ground-penetrating radar. *Permafrost Periglacial Processes* 14:319–329
- Muller SW (1947) Permafrost or permanently frozen ground and related engineering problems. J.W.Edwards, Ann Arbor, p 231
- Nelson FE, Anisimov OA, Shiklomanov NI (2001) Subsidence risk from thawing permafrost. *Nature* 410:889–890
- Osterkamp TE (2005) The recent warming of permafrost in Alaska. *Glob Planet Change* 49:187–202
- Robinson SD, Burgess MM, Kettles IM, Wolfe SA (2000) The use of ground penetrating radar in permafrost environments. In: Proceedings of the Society of Exploration Geophysics (SEG) annual conference, Calgary, pp 1363–1366
- Sazonova TS, Romanovsky VE, Walsh JE, Sergueev DO (2004) Permafrost dynamics in the 20th and 21st centuries along the east Siberian transect. *J Geophys Res* 109:D01108. doi:10.1029/2003JD003680
- Sharkhuu N (2003) Recent changes in the permafrost of Mongolia. In: Proceedings of the 8th international conference on permafrost, Zurich, Switzerland. Balkema, Lisse, pp 1029–1034
- Sharkhuu N, Sharkhuu A (2005) Recent degradation of permafrost in Mongolia. In: paper presented at first international symposium on terrestrial and climate change in Mongolia, Institute of Meteorological and Hydrological of Mongolia, Ulaanbaatar
- Singh KKK, Chauhan RKS (2002) Exploration of subsurface strata conditions for a limestone mining area in India with ground-penetrating radar. *Environ Geol* 41:966–971
- Sodnom N, Yanshin AL (1990) Geocryology and geocryological zonation of Mongolia. Digitized 2005 by Parsons M.A. National Snow and Ice Data Center/World Data Center for Glaciology, Digital Media, Boulder
- Splajt T, Ferrier J, Frostick LE (2003) Application of ground-penetrating radar in mapping and monitoring landfill sites. *Environ Geol* 44:963–967
- Vaughan DG, Hugh FJC, Christopher SMD, Waddington ED (1999) Distortion of isochronous layers in ice revealed by ground-penetrating radar. *Nature* 398:323–326
- Widess MB (1973) How thin is a thin bed? *Geophysics* 38:1176–1180
- Woo MK, Marsh P (2005) Snow, frozen soils and permafrost hydrology in Canada, 1999–2002. *Hydrol Processes* 19:215–229
- Woo MK, Winter TC (1993) The role of permafrost and seasonal frost in the hydrology of northern wetlands in North America. *J Hydrol* 141:5–31
- Wu T, Li S, Cheng G, Nan Z (2005) Using ground-penetrating radar to detect permafrost degradation in the northern limit of permafrost area on the Tibetan Plateau. *Cold Reg Sci Technol* 41:211–219
- Yang M, Wang S, Yao T, Gou X, Lu A, Guo X (2004) Desertification and its relationship with permafrost degradation in Qinghai-Xizang (Tibet) Plateau. *Cold Reg Sci Technol* 39:47–53
- Zhang T, Barry RG, Knowles K, Heginbottom JA, Brown J (1999) Statistics and characteristics of permafrost and ground-ice distribution in the northern hemisphere. *Polar Geogr* 23(2):132–154
- Zhang Y, Ishikawa M, Kadota T, Munkhtsetseg E, Oyunbaatar D, Ohata T (2004) Observational study of hydrological land-surface processes on semi-arid grassland underlain by warm permafrost in Mongolia. In: Proceedings of the 6th international study conference on GEWEX in Asia and GAME, 3–5 December, Kyoto, Japan, GAME CD-ROM Publication No. 11, T5YZ21Jul04132922
- Zhang Y, Munkhtsetseg E, Kadota T, Ohata T (2005) An observational study of ecohydrology of a sparse grassland at the edge of the Eurasian cryosphere in Mongolia. *J Geophys Res* 110:D14103. doi:10.1029/2004JD005474
- Zhang T, Nelson FE, Gruber S (2007) Introduction to special section: permafrost and seasonally frozen ground under a changing climate. *J Geophys Res* 112:F02S01. doi:10.1029/2007JF000821